

**This is the preprint version of the contribution published as:**

**Rink, K., Nixdorf, E., Zhou, C., Hillmann, M., Bilke, L. (2020):**

A virtual geographic environment for multi-compartment water and solute dynamics in large catchments

*J. Hydrol.* **582** , art. 124507

**The publisher's version is available at:**

<http://dx.doi.org/10.1016/j.jhydrol.2019.124507>

# A Virtual Geographic Environment for Multi-Compartment Water and Solute Dynamics in Large Catchments

Karsten Rink<sup>a,\*</sup>, Erik Nixdorf<sup>a</sup>, Chengzi Zhou<sup>a</sup>, Markus Hillmann<sup>b</sup>, Lars Bilke<sup>a</sup>

*<sup>a</sup>Department of Environmental Informatics, Helmholtz Centre for Environmental Research, Leipzig, Germany*

*<sup>b</sup>Wisutec Umwelttechnik GmbH, Chemnitz, Germany*

---

## Abstract

We propose a visualisation framework for data exploration, analysis and presentation of complex hydrological studies in large catchments. This furthers a deeper understanding of the interrelations between the included datasets, allows for discussions among researchers from different disciplines and is the basis for illustrating complex phenomena to stakeholders or the interested public. Based on the 162,000 km<sup>2</sup> catchment of Poyang Lake, the largest freshwater lake in China, we developed a Virtual Geographic Environment that combines a wide range of 2D and 3D observation data sets with simulation results from both an OpenGeoSys groundwater model and a COAST2D hydrodynamic model visualising water and solute dynamics within and across hydrologic reservoirs. The system aims for a realistic presentation of the investigation area and implements approaches of scientific visualisation to il-

---

\*Corresponding author at: Department of Environmental Informatics, Helmholtz Centre for Environmental Research, Leipzig, Germany

*Email address:* karsten.rink@ufz.de (Karsten Rink)

lustrate interesting aspects of multi-variate data in intuitive ways. It employs easy-to-learn interaction techniques for navigation, animation, and access to linked data sets from external sources, such as time series data or websites, to function as an environmental information system for any region of interest.

*Keywords:* Environmental Information System, Virtual Reality, OpenGeoSys, Water Resources Management, Poyang Lake

---

## 1. Motivation

For complex environmental studies, there is a considerable number of data sets required for setting up models and providing sufficient context for reliable predictions and recommendations. However, usually not all datasets can be visualised in a unified context. Researchers need to view a certain subset in geographic information systems (GIS), view time series data from observation sites online or using a dedicated plotting software and one or more modelling frameworks to view their modelling data and simulation results. Any cross-connections between these subsets have to be made mentally or manually. Such a workflow is not only prone to result in mistakes, it also complicates presenting results to stakeholders or the public in an intuitive way. In addition, considering the complex hydrological cycle and its numerous parameters and subprocesses as one typical area of application, state-of-the-art monitoring and modelling activities as well as sophisticated visualisation and data integration systems are required together to facilitate system understanding and water resources management. Particularly on the scale of entire catchments, which is appropriate for integrated management of water resources (Jaspers, 2003), the large amount of available output datasets from

19 models and remote sensing products are challenging for the development of  
20 efficient and informative visualization approaches. We propose integrating  
21 *all* datasets relevant for the analysis of a given region of interest into one uni-  
22 fied framework that serves as an Environmental Information System (EIS)  
23 for data exploration, interdisciplinary research, and knowledge transfer. We  
24 presented a first prototype for such a framework in Rink et al. (2018). For the  
25 work presented here, we use this EIS for a hydrological multi-compartment  
26 study of the Poyang Lake Basin in China. Its large size of about 162,000 km<sup>2</sup>  
27 and the complex hydrological processes within the highly dynamic lake-river-  
28 wetland system influenced by numerous drivers in the catchment, are making  
29 it an ideal study site for developing an integrated Environmental Information  
30 System for large basins.

31     Considering that about 94% of Jiangxi Province is located within Poyang  
32 Lake Basin, an improved holistic representation of the overall hydrological  
33 system and its interconnected compartments is beneficial for both the pur-  
34 suit of sustainable water resources management and for the economic con-  
35 struction and development at the provincial level. The current management  
36 system of Poyang Lake is based on the Jiangxi Poyang Lake Wetland Pro-  
37 tection Ordinance issued by the Provincial People’s Congress. The resulting  
38 system consists of a large number of authorities working independently from  
39 each other which weakens the power of both management and law enforce-  
40 ment (Fan and Hu, 2018). As a response to this situation, China is fully  
41 establishing a “river chief mechanism,” which assigns each part of a surface  
42 waterbody to an appointed official in order to improve the comprehensive  
43 management and public supervision of each basin. Consequently, integrat-

44 ing the relevant mechanisms and dynamics in the Poyang Lake Basin into  
45 a single visualisation framework has advantages with respect to evaluating  
46 future hydraulic constructions, forecasting future water quality, delineating  
47 protection zones, and mitigating environmental issues.

48 There have been previous initiatives to integrate data from different  
49 sources into a holistic visualisation platform for Poyang Lake Basin. Zhao  
50 (2018) set up a prototype system for analysing ecosystem simulation res-  
51 ults obtained with the high accuracy surface modelling method HASM (Yue,  
52 2011; Yue et al., 2015). The platform allows for the spatial-temporal analysis  
53 of raster files in the thematic areas climate change, forest carbon storage and  
54 population distribution. Gu et al. (2017) proposed a *watershed ecological vir-  
55 tual simulation and decision support platform* that combines GIS data with  
56 a 2D WATLAC hydrological model into a Virtual Geographical Environ-  
57 ment to be presented on large displays. Chen et al. (2015) integrated GIS  
58 database management systems, results from a numerical soil model and a  
59 3D Visualisation framework into a Virtual Hydrologic Environment (VHE)  
60 for Meijiang subcatchment. Zhu (2011) developed a 2D GIS environment to  
61 display hydrological data from WebGIS services and a POSTGIS database  
62 with the aim to validate the results of a two-dimensional hydrodynamic wa-  
63 ter and pollutant transport model for Poyang Lake. Similar approaches of  
64 using 2D GIS based visualization schemes for wetland data visualisation at  
65 Poyang Lake have been utilized by Zhong (2008), Xiang and Zhou (2009)  
66 and Zhao (2012) with the latter adding spatial relationship operations and  
67 their graphic representations into the developed framework. Focussing on  
68 flood inundation, Chen et al. (2012) set-up a 3D GIS system for the Poy-

ang wetlands embedding 3D structures and hydrodynamic simulation results as well as geographic objects from a object-relational database. Yan et al. (2018) developed a basic 3D environmental information system for Poyang Lake Basin. A large number of data sets, based on observation and simulation, have been included in this case study. Examples include temperature, precipitation, or ecosystem quality as well as water dynamics. However, from an implementation point-of-view the technical contribution is limited, as all data sets are imported as raster files and texture-mapped onto a 3D-model of a digital elevation model for the region.

The environmental information system (EIS) proposed here aims at creating suitable representations for all included data sets, such that the nature or certain aspects of the data are intuitively recognisable by users. Examples include the integration of precipitation data as point clouds or the simulated changes to the groundwater head as an actual triangulated plane within the 3D finite element model. This has the added advantage of being able to potentially display more data or simply remove colour as an indicator for a parameter in favour of alternative means of visualisation. In addition, we have extended the functionality of our EIS considerably and chose this case study to demonstrate both its portability to arbitrary regions of interest as well as the scalability for large volumes of data.

After a short introduction to Virtual Geographic Environments in section 2, section 3 gives an overview of the Poyang Lake Basin, including the multiple compartments included in this study. It presents details about specific data sets, modelling and simulation approaches, as well as necessary modifications during pre- and postprocessing. Section 4 gives an overview of

94 the Environmental Information System for the catchment. It shows work-  
95 flows, lists extensions to the previously presented prototype and gives ex-  
96 amples for data integration and visualisation based on specific data sets.

## 97 **2. Virtual Geographic Environments**

98 The holistic representation of all available data sets for a given region  
99 of interest is currently beyond the capabilities of established geographical  
100 information systems (GIS) such as ArcGIS or QGIS (Cox et al., 2013; Tian  
101 et al., 2016). Such frameworks have been originally designed for displaying  
102 vector- and raster-data sets. Though approaches for displaying data in 3D ex-  
103 ist, the software is usually lacking both interfaces and methods for advanced  
104 visualisation of complex three- or four-dimensional data. Examples include  
105 the representation of climate- or subsurface models, the colour-coded display  
106 of vector data to represent locally varying parameters or measurements, or  
107 the handling of time-variant data in general. On the other hand, all-purpose  
108 visualisation software such as ParaView (Ahrens et al., 2005) or VisIt (Childs  
109 et al., 2012) includes state-of-the-art visualisation techniques but lacks in-  
110 terfaces to domain-specific software such as GIS or modelling frameworks.  
111 To close this gap, we have developed the OpenGeoSys DataExplorer (Rink  
112 et al., 2013, 2014) in recent years. This software serves as a graphical user  
113 interface to the open-source modelling software OpenGeoSys (Kolditz et al.,  
114 2012a) and implements interfaces to various GIS data formats, a wide range  
115 of free and commercial modelling frameworks (for instance, FEFLOW (Dier-  
116 sch, 2014), PETREL (Schlumberger, 2018), SWMM (Rossman, 2014), Open-  
117 FOAM (Weller and Tabor, 1998)) as well as all-purpose formats such as

118 NetCDF (Rew and Davis, 1990) and VTK (Schroeder et al., 2006). The  
119 Data Explorer allows for the 3D visualisation of data via the open-source  
120 library VTK (Visualization ToolKit). The Data Explorer has been designed  
121 for the preprocessing and evaluation for numerical THM/C models, its func-  
122 tionality is insufficient for complex collaborative research projects, where the  
123 handling of large numbers of data sets can become confusing for unexperi-  
124 enced users and the implemented visualisation algorithms can be insufficient  
125 for collections of complex, possibly multi-variate or multi-modal data sets.  
126 Therefore, we recently started developing virtual geographic environments  
127 (VGE) specifically for the purpose of integrating large collections of hetero-  
128 genous data sets for the visualisation of complex environmental processes  
129 and interrelation of parameters of interest to researchers from a wide range  
130 of domains within the environmental sciences.

131 Based on the definition by Ellis (1994), the term “virtual environment”  
132 refers to an immersive, interactive experience inside a synthetic space. In re-  
133 cent years, the term has been adapted for computer-mediated communication  
134 in various domains, with “virtual learning environments” probably being the  
135 most often cited application in the media. Virtual geographic environments  
136 have been first proposed as an extension of GIS into 3D and VR (Batty,  
137 2008; Yin, 2010). Later the concept has been extended to include data from  
138 numerical models and simulation results as well as web-based data and collab-  
139 orative approaches for data interaction (Lu, 2011; Lin et al., 2013b; Kolditz  
140 et al., 2019).

141 However, our definition of a Virtual Geographic Environment slightly  
142 differs from the previously proposed framework: Lin et al. (2013a) and Lin



143 et al. (2013b) subdivide a VGE into four components: data environment,  
 144 modelling and simulation environment, interactive environment, and collab-  
 145 orative environment. In contrast, a diagram of our framework is depicted  
 146 in Fig. 1. The data life cycle starts with data added to some kind of data-  
 147 storage (e.g. a database or file storage). This data is preprocessed to remove  
 148 artifacts, calculate derived parameter sets or project it into another coordin-  
 149 ate system. That modified version of the data is either stored or forwarded  
 150 into the VGE, depending on the complexity of the selected algorithms and  
 151 the use of the processed data for other users or subsequent stages of the  
 152 workflow. Not integrating the data processing component within the VGE is  
 153 debatable, as it includes pre- and postprocessing algorithms for general data  
 154 modification (e.g. for the removal of artefacts), specific algorithms for the  
 155 modelling and simulation (e.g. for the assessment of mesh element quality  
 156 for the finite element method), specific algorithms for a subsequent visual-  
 157 isation (e.g. data reduction methods for high-dimensional multivariate data),  
 158 as well as algorithms required for both modelling and visualisation (e.g. the  
 159 projection of data into a unified coordinate system). Both, data storage and  
 160 preprocessing are what is called “data environment” in Lin et al. (2013a). If  
 161 modelling- or simulation data is part of the VGE, the (preprocessed) data  
 162 serves as input for a suitable simulation software and results are written  
 163 back to the data storage. This simulation software might be OpenGeoSys,  
 164 but as mentioned before, interfaces for files from a multitude of other software  
 165 products have been implemented as well. While this modelling/simulation-  
 166 component corresponds to the “modelling environment”, it is explicitly not  
 167 part of the VGE but simulation results are instead accessed via an interface

168 just like any other dataset. The VGE is agnostic to the origin of any data-  
169 set. As long as there is an interface to read the data it does not matter if  
170 it is research or observation data from scientific partners, state departments,  
171 companies, or data openly available on the net. Moreover, the data storage-,  
172 preprocessing-, and modelling components would work just as well without  
173 a VGE accessing the data afterwards.

174 Instead, our interpretation of a VGE consists only of a visualisation-  
175 and a presentation component, roughly corresponding to what Lin et al.  
176 (2013a) call “interactive environment” and “collaborative environment”. The  
177 visualisation component is used to create tessellated 3D objects out of envir-  
178 onmental data sets in the form of suitable metaphors or expressions (such  
179 as glyphs, streamlines, or surfaces). The presentation component includes  
180 everything required for the user experience in virtual reality, starting from  
181 the choice of shaders for 3D object and the lighting of the scene, but also  
182 animations, predefined viewpoints, picking objects to access additional in-  
183 formation, or switching objects or parameter sets live during a presentation.

184 It is worth pointing out that the workflow described above is not definit-  
185 ive. As the immersive user experience is impaired if frame rates drop below  
186 20 to 30 frames per second, it is common for complex and computationally  
187 expensive forms of visualisation to store pre-rendered representations of data-  
188 sets on a file server or database to guarantee fast rendering at all times, thus  
189 creating a direct connection of the VGE to the data storage. Also, the VGE  
190 might access the simulation component directly if *in-situ* visualisation (Bauer  
191 et al., 2016) is part of the study. However, this requires that the simulation  
192 software includes interfaces specifically designed for *in-situ* visualisation.

193 We have previously implemented the above concept for a VGE for the  
194 catchment of Chao Lake in the Anhui Province of China (Rink et al., 2018)  
195 using the OpenGeoSys Data Explorer for preprocessing data sets and em-  
196 ploying Unity (Unity Technologies, 2018), a cross-plattform game engine, for  
197 implementation. Since both pre-processing algorithms as well as the neces-  
198 sary extensions of Unity have been deliberately designed to be re-usable for  
199 future case studies, we were able to apply and extend the existing framework  
200 to build an application for the catchment of Poyang Lake presented here.

### 201 **3. Case Study Poyang Lake Basin**

#### 202 *3.1. Catchment Characteristics*

203 Poyang Lake, the largest freshwater lake in China by maximum annual  
204 extension, is located in the southeastern part of China (Fig. 2a). Annual  
205 precipitation rates in the Poyang Lake basin show a distinct wet and a dry  
206 season with a short transition period in between. Although precipitation  
207 rates are highest in June (Fig. 2b), tropical cyclones regularly cause thun-  
208 derstorms and heavy rainfall in the basin in late summer. The distribution  
209 of rainfall in its catchment controls runoff generation in the five large river  
210 systems (Ganjiang, Xinjiang, Xiushui, Raohe and Fuhe River) entering Poy-  
211 ang Lake with an basin-averaged runoff coefficient of about 0.6 (Huang et al.,  
212 2008). In addition, ungauged river systems may contribute between 12% (Li  
213 et al., 2019) and 15.6% (Du et al., 2018) of total water inflow to the lake.  
214 Poyang Lake drains into the Yangtze River at a rate of about 150 bn. m<sup>3</sup> per  
215 year which takes about 15.5% of the rivers total runoff (Zhao et al., 2011).

216 Seasonal water level variations of the lake also depend on the discharge

217 characteristics of Yangtze River and can reach more than 10 *m* at Hukou  
218 and Xingzi station between dry and wet season. At maximum extension, the  
219 water surface of the lake expands up to 3 800 km<sup>2</sup> filled by a water volume  
220 of 32 bn. m<sup>3</sup>. In addition, the fairly late yearly high water levels in Yangtze  
221 River (Fig. 2b) periodically cause a water blockage at the outflow of Poyang  
222 Lake which contributes to high water levels in the lake system (Ye et al.,  
223 2011; Yao et al., 2018). In contrast, the lake shrinks to little more than a  
224 river during the dry winter months. The corresponding change in inundation  
225 area (Hui et al., 2008) forms a unique system of water areas, wetlands and  
226 mudflats. For more details on the hydrology of the system, the interested  
227 reader is referred to the relevant publications, e.g. Li et al. (2014) and Guo  
228 et al. (2008).

229 According to the Chinese Environmental Quality Standards for Surface  
230 Water (GB3838-2002), Poyang Lake has an overall water quality that is bet-  
231 ter than most other large Chinese Lakes, such as Tai Lake or Chao Lake  
232 (Fig. 9). However, water quality is continuously deteriorating as the lake  
233 and the wetland system face several pollution pressures such as an continu-  
234 ous inflow of nutrients and fertiliser residuals from its extensively cultivated  
235 shorelines (Duan et al., 2016; Soldatova et al., 2018) as well as acidity and  
236 heavy metals from mining areas (He et al., 1998) and industrial sites (Xu and  
237 Wang, 2016). Additionally, the hydrological system is increasingly disturbed  
238 by hydraulic construction measures. The opening of the Three-Gorges-Dam  
239 (TGD) is considered one reason for generally decreasing water levels in Poy-  
240 ang Lake during the last decade (Li et al., 2017). Furthermore, prevalent sand  
241 mining activities increase water turbidity, restrict phytoplankton growth and

242 have contributed to an annual water level decrease of 1.2 to 2 m at the outflow  
243 of Poyang Lake during dry season (Lai et al., 2014; Yao et al., 2018).

244 Apart from its large size, the ecosystem of Poyang Lake is of interna-  
245 tional importance due its wide range of wetland habitats that support rich  
246 biodiversity (Huang et al., 2016; Sheng et al., 2016). For instance, many mi-  
247 gratory birds coming from Siberia, Mongolia, Japan, Korea, Northeast and  
248 Northwest China rely on these diverse habitats for overwintering, giving the  
249 ecological importance of Poyang Lake an supranational component (Yang  
250 et al., 2016).

### 251 3.2. *Preprocessing of Input Datasets*

252 As motivated in section 2, we are able to integrate a large variety of data  
253 formats into the Virtual Geographic Environment by using the OpenGeoSys  
254 Data Explorer as a preprocessing tool and exporting the data representations  
255 subsequently into Unity. For the hydrological study presented in this paper,  
256 we focussed on integrating data available on the internet. Possible sources  
257 included both websites providing monitoring data and publications providing  
258 data sets.

259 Bibliographic studies showed that a total of about 9,600 Chinese and 1,300  
260 English articles touching the topic “Poyang Lake” were published in scientific  
261 journals between 1983 to 2017 (Zhou, 2018). This includes a considerable  
262 number of publications in the field of Hydrology and Earth Sciences. How-  
263 ever, many of the published datasets lack precise information on time and  
264 location of data acquisition or have an insufficient resolution. Both are neces-  
265 sary requirements for a meaningful representation within an environmental  
266 information system. In addition, accessibility of official environmental data-

267 sets provided by local or provincial authorities in the Poyang Lake Basin is  
 268 limited. Therefore, open data from remote sensing sources as well as data  
 269 produced by physically based models of parts of the hydrological system was  
 270 used to fill data gaps in the visualisation of spatio-temporal dynamics in the  
 271 Poyang Lake Basin. Consequently, a mix of data sets from open databases,  
 272 articles, remote sensing information and official data have been integrated  
 273 into the EIS. An overview of integrated data sets is given in table 1.

### 274 *3.2.1. Surface Mapping*

275 The catchment boundary of Poyang Lake Basin was obtained by apply-  
 276 ing a GIS catchment analysis on the digital elevation model (DEM) dataset  
 277 provided by the HydroSHEDS project (Lehner et al., 2008). This dataset is  
 278 based on data from the Shuttle Radar Topography Mission (SRTM), which  
 279 has been processed for hydrological purposes. HydroSHEDs DEM defines the  
 280 elevation of the lake’s water level as constant. We modified the derived DEM  
 281 for Poyang Lake Basin for pixels actually covered by water from the lake and  
 282 replaced those values with available bathymetry data. Comparing the eleva-  
 283 tion in the non-flooded wetland areas provided by both the HydroSHEDS and  
 284 the bathymetry dataset, the average difference of elevation values was not  
 285 more than  $2\text{ m}$ , i.e. less than the vertical height accuracy of the SRTM sensors  
 286 (<https://www2.jpl.nasa.gov/srtm/statistics.html>). Due to the large  
 287 size of the Poyang Lake Basin and the requirement for a detailed reconstruc-  
 288 tion of comparatively small areas within the catchment (such as subcatch-  
 289 ments of tributaries or the lake region itself), the resulting surface mesh is  
 290 very large when considering typically used data in Unity. The complete sur-  
 291 face of the catchment consists of  $1.8 \times 10^6$  nodes and  $3.75 \times 10^6$  triangles

Table 1: Characteristics of primary data sources used within this study. Abbreviations are explained in the running text.

<b>Data type</b>	<b>Data source</b>	<b>Type</b>	<b>Spatial Resolution</b>	<b>Temporal Resolution</b>
Precipitation	GPM	Grid	0.1°	0.5 h
DEM	HydroSHEDS SRTM	Grid	3''	—
Terrain Texture	Google Earth	Grid	76.44 m (Basin) 19.11 m (Core)	—
River Network	OSM	Vector	—	—
Poyang Lake Hydrodynamics	(Du et al., 2018)	Grid	100 m	48 h
Poyang Lake Hydrochemistry	(Du et al., 2018)	Grid	100 m	48 h
Poyang Groundwater	(Nixdorf, 2018)	Grid	0.5–10 km	seasonal
Gan River Hydrochemistry	(Li et al., 2018)	Vector + Attributes	—	—
Le'an River Hydrochemistry	(Jian, 2018)	Vector + Attributes	—	seasonal
Surface Water Level	Jiangxi Water Authority	Vector + Attributes	—	—

292 with an average edge length of 500 *m*. This surface mesh has then been par-  
293 titioned into smaller meshes to allow for performance optimisation such as  
294 view-frustum culling. Technical details on suitable visualisation techniques  
295 for large geoscientific data in Unity have been presented by Rink et al. (2017).  
296 In addition to the regular surface representation, a number of refined meshes

297 have been created for certain areas of interest. Most data acquisition, sim-  
 298 ulation and visualisation efforts focus on the Poyang Core Region, which is  
 299 defined as the area of a dozen counties around Poyang Lake with a total  
 300 area of about  $19,833 \text{ km}^2$  (Tang et al., 2016). Poyang Lake is located in this  
 301 core region as well as Nanchang, the largest city in the catchment with a  
 302 population of about 3 million. Subsequently, the core region is in the focus  
 303 of this case study. The surface mesh for the core region consists of roughly  
 304  $10^6$  triangles ( $0.5 \times 10^5$  nodes) with an average edge length of  $250 \text{ m}$ . A  
 305 second, much smaller region of interest is the Dexing copper and gold mining  
 306 area located about  $100 \text{ km}$  east of Poyang Lake, which is represented by a  
 307 surface representation using just 20,000 triangles. Textures for these meshes  
 308 have been acquired from Google Earth in varying resolutions. For the Dex-  
 309 ing Mining area, we made use of Google’s “Historical view”-functionality to  
 310 create a texture-series and show the expansion of the mines from 2009 to  
 311 2018.

### 312 *3.2.2. Meteorological and Hydrological Datasets*

313 For the visualisation of precipitation, two heavy rainfall events were se-  
 314 lected from the precipitation datasets of the GPM satellite mission (Hou  
 315 et al., 2014). The first event covers the heavy rainfall caused by Typhoon  
 316 Soudelor in Southern China between 06 and 11 August 2015. A total of 287  
 317 global datasets in HDF5 format represent the time interval at a 30 minute  
 318 temporal resolution. These datasets were automatically downloaded, clipped  
 319 to the investigation area and converted into ASCII grids in the EPSG:16050  
 320 coordinate reference system using Python. A similar processing scheme was  
 321 applied for 527 precipitation grids in the time interval between the 20 and 30



322 June 2017, which represent the heavy rainfall causing the 2017 China floods  
 323 in June 2017. In addition, the location of all river gauging stations, reser-  
 324 voir gauging stations and weather stations maintained by the Jiangxi Water  
 325 Resources Department as well as the related hydrographs were included in  
 326 the EIS. The stream network of five main tributaries of Poyang Lake was  
 327 obtained from OpenStreetMaps (OSM) and classified into three orders each.  
 328 All observation sites and river geometries have been mapped onto the tri-  
 329 angulated three-dimensional surface generated from the DEM using a linear  
 330 interpolation algorithm proposed in Rink et al. (2014). In addition, the res-  
 331 ults of a two-dimensional hydrodynamic lake model (Du et al., 2018) were  
 332 integrated into the EIS to visualise inundation changes as well as water and  
 333 matter transport in Poyang Lake (see Fig. 5). The provided dataset consist of  
 334 186 rasters representing the temporal dynamics in the lake between Septem-  
 335 ber 2009 to February 2011 with a temporal resolution of  $\sim 2.1$  days. We  
 336 implemented a reader to convert the COAST2D simulation output into the  
 337 VTK unstructured grid format. Specifically, each time step would be writ-  
 338 ten to a separate file, with each parameter represented by an array within  
 339 that file. As a result, we ended up 186 mesh files, each consisting of 47,000  
 340 quad elements and containing information on flow direction, flow velocity  
 341 and four chemical concentrations for each cell. Given that representation,  
 342 it is straightforward to display a temporal sequence for any of the included  
 343 parameters and use VTK for subsequently applying visualisation algorithms  
 344 to the data set.

345 To represent the groundwater flow system, the distribution of hydraulic  
 346 heads, groundwater velocities and stream path trajectories in the Poyang

347 Lake Basin has been visualised in the EIS based on the results of the ground-  
 348 water model developed by Nixdorf (2018) (see Fig. 6). The groundwater re-  
 349 gime was simulated in two-dimensional planar direction for low and high wa-  
 350 ter levels in Poyang Lake using the open source THMC FEM code OpenGeo-  
 351 SyS (Kolditz et al., 2012a), which has been applied for groundwater flow sim-  
 352 ulations on the regional scale under various scientific objectives in previous  
 353 studies (e.g. Walther et al. (2014); Wu et al. (2011); Nixdorf et al. (2017)).  
 354 The two-dimensional triangular FEM mesh used for the simulation consists  
 355 of about 150,000 Elements with a spatial resolution of about 500 *m* inside  
 356 and about 10 *km* outside of the Poyang Lake Core Region (for details of the  
 357 model pre- and postprocessing see Nixdorf (2018)). The groundwater flow  
 358 model computes hydraulic head (Fig. 6a) and groundwater velocity vectors  
 359 (Fig. 6b) at each node/element of the FEM mesh for December 1999 (low  
 360 lake water level) and September 2000 (high water level) in VTK format, for  
 361 subsequent integration into the EIS system.

### 362 3.2.3. *Hydrochemistry*

363 In general, public information on water quality of surface waters – in-  
 364 cluding meta-data on sampling location and time – are difficult to obtain for  
 365 Chinese water bodies. Accessible datasets are rarely available in a sufficient  
 366 spatial resolution, particularly if the investigation aims to focus on large river  
 367 networks (Nixdorf et al., 2015). However, recently a number of studies has  
 368 been published, providing data on surface water pollution caused by min-  
 369 ing activities monitored along tributaries of Poyang Lake. He et al. (2018)  
 370 measured surface water contents of arsenic, chromium, copper, uranium and  
 371 thorium at 13 sampling sites in Fu River as well as in its tributary Lin River.

Jian (2018) investigated seasonal changes of heavy metal concentration (copper, lead and cadmium) in the water, soil and sediments at 13 sampling sites of Le'an River, which is a tributary of Xin River, in order to reveal the impact of the Dexing mining area on the stream ecosystem. The results of this study were included in the EIS together with the study of Li et al. (2018), who measured dissolved concentrations of 15 different heavy metals at 37 locations covering the entire Gan River network. For the EIS, we limited ourselves to two prototypical representations for the chemical data: (1) For Le'an River, we display a spatio-temporal distribution for the concentration of copper in the river during various seasons (the pollution during wet season is shown in Fig. 9c). (2) For the Gan River network, we included a multivariate dataset for a fixed point in time, allowing the user to switch through a linearly interpolated mapping of the 15 metal concentrations (see Fig. 7). The visualisation of chemical concentration in 3D river representations has been kept simple on purpose, to allow domain scientists to intuitively understand the displayed data. The combination of both temporal and multivariate data is not a technical issue, but the two dimensional parameter space (compound vs time) becomes difficult to navigate without a specifically designed user interface. Likewise, a concurrent visualisation of multivariate data, such as via glyphs or small multiples, is not straightforward to understand without being given instructions.

Hydrochemical data for Poyang Lake were integrated in the EIS based on the two-dimensional lake model of Du et al. (2018). The simulation includes information on the distribution and dynamics of total phosphorus, total nitrogen, ammoniacal nitrogen and the permanganate index in Poyang Lake in

397 a spatial-temporal resolution of 100 *m* and  $\sim 2.1$  days, respectively. This is  
398 identical to the hydrodynamic dataset mentioned previously; see conversion  
399 details in section 3.2.2.

#### 400 **4. Construction of the Poyang Lake VGE**

401 In Rink et al. (2018), we proposed a framework for creating Virtual Geo-  
402 graphic Environments using Unity as well as a workflow for preparing the  
403 data to be included. An illustration of the workflow is shown in Fig. 8 and  
404 we will give a brief outline in the following: Based on the intended purpose  
405 of the VGE, datasets to be included are selected based on availability and  
406 their usefulness in the scope of the case study. Datasets often require prepro-  
407 cessing for fitting seamlessly together with other available datasets. While  
408 modification of the data (or their graphical representation) is possible at a  
409 later stage of the workflow, it is recommended to use the software products  
410 the datasets have been created with as much as possible to preserve the data's  
411 inherent structure and parameters, and avoid the creation of processing arte-  
412 facts. A typical example is using a Geographical Information System for  
413 the projection of all datasets into the same coordinate system. Once pre-  
414 pared, all datasets are imported into a VTK-based processing software such  
415 as the OGS Data Explorer or ParaView, where graphical representations  
416 of each dataset are created. While ParaView is an all-purpose software for  
417 scientific visualisation, the Data Explorer offers a number of interfaces and  
418 algorithms specifically developed for the handling of environmental datasets.  
419 Either framework is used to modify the data in ways that have either not  
420 been supported in the original software or which are specific to the graphical

421 representation of the data. An example of this is the mapping of a raster file  
 422 (e.g. remote sensing imagery) onto a warped surface representing the region  
 423 of interest. Also at this stage, artefacts are handled, and data reduction  
 424 algorithms are used to adequately prepare datasets for visualisation. Dur-  
 425 ing the visualisation-stage, suitable representations for each of the datasets  
 426 will be selected and visualisation algorithms are applied so the interesting  
 427 aspects of each datasets will become visible or emphasised. Suitable colours  
 428 and transfer functions are selected, if possible in such a way that the colours  
 429 will help users to understand the data. Finally, the finished graphical objects  
 430 representing the original datasets will be imported into the Unity framework  
 431 where parameters concerning the rendering within the scene will be set. At  
 432 the lowest level, this includes selecting light sources for the scene or assigning  
 433 specific shaders to a datasets (Bailey and Cunningham, 2011) (i.e. defining  
 434 how the dark, shiny, or colourful the object will appear, as well as setting  
 435 more elaborate rendering effects). In addition, presentation-specific function-  
 436 ality is set up. This includes viewpoints of positions in 3D space the user can  
 437 select from a menu and will automatically be guided to, picking objects to  
 438 receive additional information (we can link images (Fig. 4), movies or docu-  
 439 ments or even interactive graphs to any 3D object), selecting and controlling  
 440 animations via control menu, or switching simulation scenarios.

441 As an specific example, we would like to illustrate the above workflow  
 442 based on the dataset for Le'an river: The course of the 280 *km* long river  
 443 is part of the Chinese river network dataset acquired from OpenStreetMap.  
 444 The data is imported into QGIS, the river has been extracted and projected  
 445 into the EPSG:16050 (UTM zone 50N) coordinate system used for this case

446 study (Fig. 9a). The river dataset has then been saved into the shapefile  
 447 vector format and imported into the OpenGeoSys Data Explorer. Here,  
 448 adjacent points with a distance of less than  $100\text{ m}$  to each other have been  
 449 removed. This reduces the size of the dataset by more than  $50\%$  without the  
 450 difference being visible to the human eye due to the size of study area and  
 451 the final representation of the river. Now, the dataset is mapped onto the 3D  
 452 representation of the DEM, so it fits into the geographic context of the case  
 453 study (Fig. 9b). We applied a VtkTubeFilter, changing the representation of  
 454 the polyline-vector-data into a triangulated pipe-like structure with a radius  
 455 of  $50\text{ m}$ . This is required because the original line structure will always  
 456 be rendered at a width of one pixel and is thus too inconspicuous to be  
 457 noticed. The dataset was assigned the colour blue, a colour that is typically  
 458 associated with water. At each point of the dataset we now added scalar  
 459 values representing the copper-concentration at different times of the year,  
 460 acquired via Jian (2018). The higher the concentration, the more the colour  
 461 of the associated river-segment will turn red. This colour is especially suitable  
 462 here, not only because red is usually associated as a warning or sign of danger,  
 463 but the severely high concentration of the copper *actually* gives the river a  
 464 reddish-brown colour. The transfer function we applied turns yellow at a  
 465 concentration of  $1\text{ mg/l}$ , red at  $2\text{ mg/l}$  and violet at  $3\text{ mg/l}$ . We then exported  
 466 the dataset into the Autodesk FBX format, which can be employed to import  
 467 data into Unity. Location, mapping and colour are automatically adopted  
 468 during this process. In Unity, we parameterised the dataset such that it is  
 469 rendered using a simply Gouraud-shader without casting shadows (which is  
 470 not necessary as it is being located on the catchment surface) and rendering

471 backfaces (located at the inner side of the tube) in order to save computing  
472 power. An animation was defined to change the colour of the dataset based  
473 on the copper-concentration during different times of the year (Fig. 9c), in  
474 addition the user can access images of river to get a less abstract view of the  
475 situation. A viewpoint was set near Dexing Mine where the Copper enters  
476 the river. As a result, that particular point-of-view can be set automatically  
477 during a presentation, and an interpolated path along the river will guide  
478 the user from Dexing Mine to Poyang Lake.

479 Depending on the complexity of each of the included datasets, some of  
480 the steps described above may not be necessary or other algorithms might  
481 need to be applied instead. It's important to note that all of the required  
482 algorithms are implemented in OGS, ParaView or Unity and can be executed  
483 via user dialogues in the respective software programme, thus significantly  
484 reducing the time required for each of the steps. It is worth pointing out that  
485 the workflow shown in Fig. 8 is a subset of the data workflow introduced by  
486 Kolditz et al. (2012b), based on the structure shown in Fig. 1.

487 In addition to what had been presented in Rink et al. (2018), the func-  
488 tionality of our framework has been expanded for handling a number of types  
489 of datasets that will be presented here briefly:

490 Previously, it has only been possible to assign transfer functions based on  
491 spatial-temporal parameters of FEM-based simulation results. These trans-  
492 fer functions assign (and can interpolate) colour values to encode additional  
493 information during the presentation. A generalisation of that algorithm now  
494 also allows the assignment of data to geometrical data in OpenGeoSys and  
495 has been used, as described above, to visualise the changing concentration

of various chemical compounds in Poyang Lake and its tributary rivers. As demonstrated by Samsel et al. (2017) (and more generalised in Zhou and Hansen (2016)), suitable colour maps and transfer functions are of vital importance for an intuitive understanding of visually presented data. As such, we are using applications such as ParaView (Ahrens et al., 2005) or ColorBrewer (Harrower and Brewer, 2011) to generate colour lookup tables (LUT) that are either based on specific values or ranges (such as the LUTs in Fig. 7 and 9c, based on permissible/critical values for Copper concentration in drinking water) or that can be adequately discriminated with human perception.

We also created animations from remote sensing data acquired over multiple years: Google Earth imagery from 2009 to 2018 is used as texture for the Dexing mining area. It shows topographical changes of area and adds to the visualisation of the water pollution in Le'an river discussed above. As such, it enriches the understanding for a user exploring the data via the Environmental Information System and serves the holistic approach of the framework.

To visualise the hydrological processes simulated via COAST2D and OpenGeoSys and discussed in Section 3.2, we applied and adjusted algorithms provided by VTK: For the groundwater simulation, triangle nodes have been mapped to the elevation of the groundwater head, thus creating a warped surface of the simulated water level. In addition, arrow-glyphs have been generated, where the direction of arrow indicates flow direction and the colour the simulated velocity. A total of 10,000 arrows positioned on an equilateral grid have been calculated and mapped onto the surface representing the



521 groundwater head for low and higher water level, each (see Fig. 6b). For  
522 the surface water hydraulics of the Poyang Lake, a streamline representation  
523 of the flow was selected. Given the complex and drastically changing area  
524 covered by the lake and large variations in velocity, representing flow via  
525 arrow-glyphs as with the groundwater model results in a confusing visualisa-  
526 tion where glyphs are not necessarily located on the lake surface and larger  
527 glyphs may conceal smaller ones. In contrast, streamlines preserve the shape  
528 of the original graphical object and are a suitable way to visualise eddies in  
529 the water (see Fig. 5a).

530 During a concurrent visualisation of both surface and groundwater flow,  
531 the different modes of representation also allow to easily differentiate between  
532 data sets. Integrating surface and subsurface water flow fields in one visu-  
533 alisation helps to reveal the complex spatio-temporal pattern of gaining and  
534 losing conditions along the lake’s shoreline and subsequently may facilit-  
535 ate the understanding of cross-compartment interaction in the Poyang Lake  
536 Basin.

537 In previous studies, we have relied on the visualisation of diagrams for  
538 time series of weather and climate data. Here, the occurrence of large storms  
539 and extreme rain events required a different representation to meet the re-  
540 quest for a multi-compartment approach for hydrological processes. Exem-  
541 plary data from two extreme weather events (see section 3.2.2) have been  
542 used to implement an algorithm for the 3D representation of precipitation  
543 data. Given 288–528 raster data sets of precipitation intensity per rain event,  
544 we created a point cloud representation for visualising rain. Each pixel  
545  $p_i$  from the raster data is given an adjustable height-parameter and thus

546 forms a bounding box  $B_i$  in 3D space. Within  $B_i$ ,  $n_{ij}$  points are randomly  
 547 seeded, with  $n_{ij}$  being dependent on the amount of precipitation on pixel  $p_i$   
 548 at timestep  $t_j$ . Colours can be adjusted based on height, intensity, or any  
 549 other parameter derived from the dataset. The result is a vivid impression  
 550 of rain clouds moving over the region of interest (see Fig. 10).

551 While such animations are very intuitive, we did also include diagrams  
 552 showing time series data from observation sites, to allow experts to verify  
 553 numbers and assess the development of the observed events. For intuitive  
 554 access, the available timeseries data is linked to the representation of ob-  
 555 servation sites in the 3D scenes. If these objects are picked via mouse or  
 556 flystick, a 2D overlay window opens, displaying the time series for that par-  
 557 ticular site as a diagram. For this case study, we also added an interface to the  
 558 AL.VIS/Timeseries framework developed by the *WISUTEC Umwelttechnik*  
 559 *GmbH*, one of our cooperation partners during the project. This interface al-  
 560 lows online-access to the AL.VIS database and shows current measurements  
 561 at the selected observation site (Fig. 11). AL.VIS/Timeseries is able to im-  
 562 port data from different sources for quality assurance, research, analysis and  
 563 exporting. The used database model is very flexible and can process very  
 564 long time series with more than  $10^6$  measured values very fast. Multiple  
 565 diagrams linked to observation sites in the VGE can be opened concurrently  
 566 and allow users to investigate the time series data interactively via pan and  
 567 zoom functionality.

568 Due to the large extent of the Poyang Lake Basin, we encountered a  
 569 number of new challenges concerning the VGE for this region. The most  
 570 challenging issue was related to data volume: A sufficiently fine resolution is

necessary to realistically depict areas of interest and to ensure that geographic features such as river valleys are rendered correctly. This was of special importance due to the requirement for spatio-temporal visualisation of rivers and their pollution in the correct geographical context. Given the size of the catchment, both surface grids and texture data is reasonably large. However, for an interactive and immersive VR application, a sufficiently high frame-rate is required so users won't experience stuttering during animations or missing time steps in the rendering of simulation results. Fortunately, recent versions of the Unity engine support not only very large texture-sizes, but also level-of-detail approaches, where multiple resolutions of surface grids are assembled into a tree structure and cross-fading between data sets is automatically handled by Unity itself. In addition, we included river network representations with a varying number of tributaries included as well as varying diameter of tube-representations of rivers. In addition, we use standard procedures for saving rendering time by making use of backface culling (i.e. only the front-faces of triangles are rendered) or view frustum culling (i.e. only currently visible objects are rendered). Another issue is related to the visibility of small (or thin) structures within a large context. We have addressed this issue before, but due to the size of the catchment it was of special importance in this case study. For an overview of the river network, it required different representations of rivers, as mentioned before. A large diameter of tube structures is required for the objects to be clearly visible when showing the whole catchment. However, a much smaller representation is needed when zooming in on certain regions of interest. Here, we solved the issue by linking specific representations of datasets to given predefined

viewpoints. If the user is selecting a viewpoint that will show large parts of the catchment, larger representations of the rivers with fewer tributaries are shown. If a viewpoint close to the surface is selected, those datasets become transparent and instead a finer resolution with more tributaries is rendered. The same approach is used for small regions of interest such as the Dexing mining area.

We have used the proposed framework to present complex data collections to a wide range of audiences. The 3D visualisation of multi-compartment data has proven to be an excellent means to present research questions and progress to both stakeholders and the interested public, allowing to present complex processes and relationships in an easy-to-understand and engaging way. The virtual reality approach fosters discussions between collaborating scientists by allowing an in-depth look at data characteristics with a complex context. In our Lab (Bilke et al., 2014), we use MiddleVr as a Unity plug-in to present this case study in our Virtual Reality environment using  $6 \times 3\text{ m}$  video wall with additional projections on both sides as well as the floor (Fig. 12). The system is powered by 13 beamers and users are tracked via an array of nine infrared cameras, thus providing an immersive environment during presentations. Users can interact with the scene via a flystick or a gamepad. However, MiddleVr also supports a multitude of other platforms and we have built our applications for regular PCs as well as for head-mounted displays such as the HTC Vive or the Oculus Rift.

## 618 5. Conclusions

619 We presented a holistic analysis of water and solute dynamics in a large  
620 catchment, highlighting the importance of visualisation for analysing and un-  
621 derstanding complex data collections and simulation results. A wide range  
622 of observation data in vector- and raster format have been converted into  
623 3D models and are complemented by previously published simulation results  
624 of a groundwater flow model for the Poyang Lake Basin as well as a solute  
625 transport model of the lake itself. All data sets have been projected into  
626 a unified geographical context for a complementary visualisation within a  
627 Virtual Geographic Environment. Highlighting points of interest and visual-  
628 ising phenomena relevant to a hydrological analysis of the region facilitates  
629 a deeper understanding of the underlying processes and allows a visual cor-  
630 relation of the integrated data. Additional information such as time series,  
631 imagery, or websites is linked to corresponding objects in the scene, creating  
632 a 3D Environmental Information System for the Poyang Lake Basin. The  
633 application allows for interactive data exploration in Virtual Reality, both  
634 in cave-like environments or using head-mounted displays, but can also be  
635 run on regular personal computers. The software frameworks used and the  
636 algorithms developed are in no way limiting the application to the presented  
637 case study and can be easily applied to other regions of interest. This form of  
638 presentation gives researchers a comprehensive view of all relevant data sets  
639 for any given case study, allows for interdisciplinary discussions between col-  
640 laborating scientists, supplements presentations of research results and has  
641 been successfully used for knowledge transfer during open day events.

## 642 **Acknowledgements**

643 This work, being a part of the Sino-German cooperation group project  
644 “A modelling platform prototype for environmental system dynamics”, is fun-  
645 ded by Sino-German Centre for Science Promotion (CDZ). The funding un-  
646 der grant GZ1167 (T533D810) is greatly acknowledged. Additional funding  
647 came from the Helmholtz Association through the projects “Advanced Earth  
648 System Modelling Capacity" and "Digital Earth". We would like to thank  
649 Tianxiang Yue from the Institute of Geographical Sciences and Natural Re-  
650 sources and Yanliang Du from the China Institute of Water Resources and  
651 Hydropower Research for data support. This work is based on concepts de-  
652 veloped in the scope of the project “Managing Water Resources for Urban  
653 Catchments” (grant number 02WCL1337A).

## 654 **References**

- 655 Ahrens, J., Geveci, B., Law, C., 2005. ParaView: An End-User Tool for Large  
656 Data Visualization, in: Hansen, C., Johnson, C. (Eds.), The Visualization  
657 Handbook. Elsevier.
- 658 Bailey, M., Cunningham, S., 2011. Graphic Shaders: Theory and Practice.  
659 2nd ed., CRC Press.
- 660 Batty, M., 2008. Virtual reality in Geographic Information Systems, in:  
661 Wilson, J., Fotheringham, A. (Eds.), The Handbook of Geographic In-  
662 formation Science. Blackwell Publishing, Oxford, UK, pp. 317–334.
- 663 Bauer, A.C., Abbasi, H., Ahrens, J., et al., 2016. In Situ Methods, Infra-

664 structures, and Applications on High Performance Computing Platforms.  
665 Comput Graph Forum 35, 577–597. doi:10.1111/cgf.12930.

666 Bilke, L., Fischer, T., Helbig, C., et al., 2014. TESSIN VISLab – Laboratory  
667 for Scientific Visualization. Environ Earth Sci 72, 3881–3899. doi:10.  
668 1007/s12665-014-3785-5.

669 Chen, C., Sun, F., Kolditz, O., 2015. Design and integration of a gis-based  
670 data model for the regional hydrologic simulation in meijiang watershed,  
671 china. Environmental Earth Sciences 74, 7147–7158.

672 Chen, J., Wu, X., Wang, Z., Zhu, J., 2012. Establishment of fundamental  
673 geographic information system and associated key technologies for poyang  
674 lake wetland. Geomatics and Information Science of Wuhan University 37.  
675 In Chinese.

676 Childs, H., Brugger, E., Whitlock, B., et al., 2012. VisIt: An End-User  
677 Tool For Visualizing and Analyzing Very Large Data, in: High Per-  
678 formance Visualization–Enabling Extreme-Scale Scientific Insight. CRC  
679 Press/Francis–Taylor Group, pp. 357–372.

680 Cox, M.E., James, A., Hawke, A., Raiber, M., 2013. Groundwater visu-  
681 alisation system (gvs): A software framework for integrated display and  
682 interrogation of conceptual hydrogeological models, data and time-series  
683 animation. Journal of Hydrology 491, 56–72.

684 Diersch, H.J.G., 2014. FEFLOW – Finite Element Modeling of Flow, Mass  
685 and Heat Transport in Porous and Fractured Media. Springer, Berlin,  
686 Heidelberg.

- 687 Du, Y., Peng, W., Wang, S., et al., 2018. Modeling of water quality evolu-  
688 tion and response with the hydrological regime changes in Poyang Lake.  
689 Environ Earth Sci 77, 265. doi:10.1007/s12665-018-7408-4.
- 690 Duan, W., He, B., Nover, D., et al., 2016. Water Quality Assessment and  
691 Pollution Source Identification of the Eastern Poyang Lake Basin Using  
692 Multivariate Statistical Methods. Sustainability 8, 133. doi:10.3390/  
693 su8020133.
- 694 Ellis, S.R., 1994. What are virtual environments? IEEE Comput Graph  
695 Appl 14, 17–22. doi:10.1109/38.250914.
- 696 Fan, Z., Hu, Z., 2018. Strengthening integrated management and maintaining  
697 the health of Poyang Lake, in: Chinese Water Systems – Poyang Lake.  
698 Springer, pp. 41–51.
- 699 Feng, L., Han, X., Hu, C., Chen, X., 2016. Four decades of wetland changes of  
700 the largest freshwater lake in China: Possible linkage to the Three Gorges  
701 Dam? Remote Sens Environ 176, 43–55. doi:10.1016/j.rse.2016.01.  
702 011.
- 703 Gu, S., Fang, C., Wang, Y., 2017. Virtual geographic environment for WAT-  
704 LAC hydrological model integration, in: Proc of 25th International Con-  
705 ference on Geoinformatics, IEEE Computer Society.
- 706 Guo, H., Hu, Q., Jiang, T., 2008. Annual and seasonal streamflow re-  
707 sponses to climate and land-cover changes in the Poyang Lake basin, China.  
708 Journal of Hydrology 355, 106–122. doi:10.1016/j.jhydrol.2008.03.  
709 020.



- 710 Guo, H., Hu, Q., Zhang, Q., Feng, S., 2012. Effects of the Three Gorges  
711 Dam on Yangtze River flow and river interaction with Poyang Lake, China:  
712 2003-2008. *J Hydrol* 416–417, 19–27. doi:10.1016/j.jhydrol.2011.11.  
713 027.
- 714 Harrower, M., Brewer, C.A., 2011. ColorBrewer.org: An Online Tool for  
715 Selecting Colour Schemes for Maps, in: Dodge, M., Kitchin, R., Perkins, C.  
716 (Eds.), *The Map Reader: Theories of Mapping Practice and Cartographic*  
717 *Representation*. Wiley. doi:[https://doi.org/10.1002/9780470979587.](https://doi.org/10.1002/9780470979587.ch34)  
718 ch34.
- 719 He, L., Gao, B., Luo, X., et al., 2018. Health Risk Assessment of Heavy  
720 Metals in Surface Water near a Uranium Tailing Pond in Jiangxi. *Sustain-*  
721 *ability* 10, 1113. doi:10.3390/su10041113.
- 722 He, M., Wang, Z., Tang, H., 1998. The chemical, toxicological and ecological  
723 studies in assessing the heavy metal pollution in Le An River, China. *Water*  
724 *Res* 32, 510–518. doi:10.1016/S0043-1354(97)00229-7.
- 725 Hou, A.Y., Kakar, R.K., Neeck, S., et al., 2014. The global precipitation  
726 measurement mission. *Bull Am Meteorol Soc* 95, 701–722.
- 727 Huang, X., Hu, B., Wang, P., et al., 2016. Microbial diversity in lake–river  
728 ecotone of Poyang Lake, China. *Environ Earth Sci* 75, 965. doi:10.1007/  
729 s12665-016-5473-0.
- 730 Huang, Y., Xu, G., Shen, Y., Xu, Z.Q.C., 2008. Research on analysis methods  
731 of water resources quantity balance in plain river- net areas. *Yangtze River*  
732 39, 24–27.

733 Hui, F., Xu, B., Huang, H., et al., 2008. Modelling spatial-temporal change  
734 of Poyang Lake using multitemporal Landsat imagery. *Int J Remote Sens*  
735 29, 5767–5784. doi:10.1080/01431160802060912.

736 Jaspers, F.G., 2003. Institutional arrangements for integrated river basin  
737 management. *Water Pol* 5, 77–90.

738 Jian, M., 2018. Distribution of aquatic macrophytes in the Leán River  
739 and its indicative evaluation on heavy metal pollution. In: *Chinese Wa-*  
740 *ter Systems- Poyang Lake*, in: *Chinese Water Systems – Poyang Lake*.  
741 Springer, pp. 139–184.

742 Jiangxi Water Resources Department, 2013. *Jiangxi Water Resources Bul-*  
743 *letin* 2013.

744 Kolditz, O., Bauer, S., Bilke, L., et al., 2012a. OpenGeoSys: An open source  
745 initiative for numerical simulation of thermo-hydro-mechanical/chemical  
746 (THM/C) processes in porous media. *Environ Earth Sci* 67, 589–599.  
747 doi:10.1007/s12665-012-1546-x.

748 Kolditz, O., Rink, K., Nixdorf, E., et al., 2019. Environmental Information  
749 Systems: Paving the Path for Digitally Facilitated Water Management  
750 (Water 4.0). *Engineering (accepted)*.

751 Kolditz, O., Rink, K., Shao, H., et al., 2012b. International viewpoint and  
752 news: data and modelling platforms in environmental earth sciences. *En-*  
753 *viron Earth Sci* 66, 1279–1284. doi:10.1007/s12665-012-1661-8.

754 Lai, X., Shankman, D., Huber, C., et al., 2014. Sand mining and increasing  
755 Poyang Lake’s discharge ability: A reassessment of causes for lake decline

756 in China. *J Hydrol* 519, 1698–1706. doi:10.1016/j.jhydrol.2014.09.  
757 058.

758 Lehner, B., Verdin, K., Jarvis, A., 2008. New Global Hydrography Derived  
759 From Spaceborne Elevation Data. *Eos, Trans Am Geophys Union* 89, 93–  
760 104. doi:10.1029/2008E0100001.

761 Li, C., Wang, P., Chen, B., Li, Y., 2018. Spatial distribution and pollution  
762 source of dissolved metals in the Ganjiang River of Lake Poyang Basin. *J*  
763 *Lake Sci* 30, 139–149.

764 Li, Y., Zhang, Q., Liu, X., Yao, J., 2019. Water balance and flashiness for  
765 a large floodplain system: A case study of Poyang Lake, China. *Sci Total*  
766 *Environ* doi:10.1016/j.scitotenv.2019.135499.

767 Li, Y., Zhang, Q., Werner, A.D., et al., 2017. The influence of river-to-lake  
768 backflow on the hydrodynamics of a large floodplain lake system (Poyang  
769 Lake, China). *Hydrol Process* 31, 117–132. doi:10.1002/hyp.10979.

770 Li, Y., Zhang, Q., Yao, J., Werner, A.D., Li, X., 2014. Hydrodynamic and  
771 hydrological modeling of the Poyang Lake catchment system in China.  
772 *Journal of Hydrologic Engineering* 19, 607–616.

773 Lin, H., Chen, M., Lu, G., 2013a. Virtual Geographic Environment: A  
774 Workspace for Computer-Aided Geographic Experiments. *Ann Assoc Am*  
775 *Geogr* 103, 465–482.

776 Lin, H., Chen, M., Lu, G., et al., 2013b. Virtual Geographic Environments  
777 (VGEs): A New Generation of Geographic Analysis Tool. *Earth Sci Rev*  
778 126, 74–84.

- 779 Lu, G.N., 2011. Geographic Analysis-oriented Virtual Geographic Envir-  
780 onment: Framework, Structure and Functions. *Sci China Earth Sci* 54,  
781 733–743. doi:10.1007/s11430-011-4193-2.
- 782 Nixdorf, E., 2018. Modelling seasonal groundwater flow dynamics in the  
783 Poyang Lake Core Region, in: *Chinese Water Systems – Poyang Lake*.  
784 Springer, pp. 69–94.
- 785 Nixdorf, E., Chen, C., Sun, Y., Kolditz, O., 2015. Persistent organic pollut-  
786 ants contaminate Chinese water resources: overview of the current status,  
787 challenges and European strategies. *Environ Earth Sci* 74, 1837–1843.  
788 doi:10.1007/s12665-015-4448-x.
- 789 Nixdorf, E., Sun, Y., Lin, M., Kolditz, O., 2017. Regional assessment of  
790 groundwater contamination risk in the Songhua River Basin, China, by  
791 integrating public data sets, web services and numerical modelling tech-  
792 niques. *Sci Total Environ* 605–606, 598–609.
- 793 Rew, R., Davis, G., 1990. NetCDF: an interface for scientific data access.  
794 *IEEE Comp Graph and App* 10, 4.
- 795 Rink, K., Bilke, L., Kolditz, O., 2014. Visualisation Strategies for Environ-  
796 mental Modelling Data. *Environ Earth Sci* 72, 3857–3868. doi:10.1007/  
797 s12665-013-2970-2.
- 798 Rink, K., Bilke, L., Kolditz, O., 2017. Setting up Virtual Geographic  
799 Environments in Unity, in: *Proc. of EuroVis Workshop on Visualiza-*  
800 *tion in Environmental Sciences*, EuroGraphics Digital Library. pp. 1–5.  
801 doi:10.2312/envirvis.20171096.

802 Rink, K., Chen, C., Bilke, L., et al., 2018. Virtual geographic environments  
803 for water pollution control. *Int J Dig Earth* 11, 397–407. doi:10.1080/  
804 17538947.2016.1265016.

805 Rink, K., Fischer, T., Selle, B., Kolditz, O., 2013. A Data Exploration  
806 Framework for Validation and Setup of Hydrological Models. *Environ*  
807 *Earth Sci* 69, 469–477. doi:10.1007/s12665-012-2030-3.

808 Rossman, L., 2014. SWMM-CAT User’s Guide. Technical Report EPA 600-  
809 R-14-428. United States Environmental Protection Agency.

810 Samsel, F., Turton, T.L., Wolfram, P., Bujack, R., 2017. Intuitive Colormaps  
811 for Environmental Visualization, in: *Proc. of EuroVis Workshop on Visu-*  
812 *alization in Environmental Sciences*, EuroGraphics Digital Library. pp.  
813 55–59. doi:10.2312/envirvis.20171105.

814 Schlumberger, 2018. Petrel E&P Software Platform. [https://www.](https://www.software.slb.com/products/petrel)  
815 [software.slb.com/products/petrel](https://www.software.slb.com/products/petrel). Accessed: 2018-08-30.

816 Schroeder, W., Martin, K., Lorensen, B., 2006. Visualization Toolkit: An  
817 Object-Oriented Approach to 3D Graphics (4th Edition). Kitware, Inc.

818 Sheng, P., Yu, Y., Zhang, G., et al., 2016. Bacterial diversity and distribution  
819 in seven different estuarine sediments of Poyang Lake, China. *Environ*  
820 *Earth Sci* 75, 479. doi:10.1007/s12665-016-5346-6.

821 Soldatova, E., Sun, Z., Maier, S., et al., 2018. "shallow groundwater quality  
822 and associated non-cancer health risk in agricultural areas (poyang lake  
823 basin, china)". *Environ Geochem Health* 40, 2223–2242. doi:10.1007/  
824 s10653-018-0094-z.

825 Tang, X., Li, H., Xu, X., et al., 2016. Changing land use and its impact on  
826 the habitat suitability for wintering Anseriformes in China's Poyang Lake  
827 region. *Sci Total Environ* 557–558, 296–306. doi:10.1016/j.scitotenv.  
828 2016.03.108.

829 Tian, Y., Zheng, Y., Zheng, C., 2016. Development of a visualization tool for  
830 integrated surface water–groundwater modeling. *Comput Geosci* 86, 1–14.

831 Unity Technologies, 2018. Unity (Version 2018.3). <https://unity3d.com/>.

832 Walther, M., Bilke, L., Delfs, J.O., et al., 2014. Assessing the saltwater re-  
833 mediation potential of a three-dimensional, heterogeneous, coastal aquifer  
834 system: Model verification, application and visualization for transient  
835 density-driven seawater intrusion. *Environ Earth Sci* 72, 3827–3837.  
836 doi:10.1007/s12665-014-3253-2.

837 Weller, H.G., Tabor, G., 1998. A tensorial approach to computational con-  
838 tinuum mechanics using object-oriented techniques. *Comput Phys* 12, 620–  
839 631. doi:10.1063/1.168744.

840 Wu, Y., Wang, W., Toll, M., et al., 2011. Development of a 3D groundwater  
841 model based on scarce data: The Wadi Kafrein catchment/Jordan. *Environ*  
842 *Earth Sci* 64, 771–785. doi:10.1007/s12665-010-0898-3.

843 Xiang, S., Zhou, W., 2009. Design and development of water environmental  
844 geographic information system in poyang lake. *Journal of East China*  
845 *Jiaotong University*, 4In Chinese.

846 Xu, B., Wang, G., 2016. Surface water and groundwater contamina-  
847 tions and the resultant hydrochemical evolution in the Yongxiu area,

848 west of Poyang Lake, China. *Environ Earth Sci* 75, 184. doi:10.1007/  
849 s12665-015-4778-8.

850 Yan, C., Rink, K., Bilke, L., et al., 2018. Virtual geographical environment-  
851 based environmental information system for Poyang Lake Basin, in:  
852 Chinese Water Systems – Poyang Lake. Springer, pp. 41–51.

853 Yang, P., Liu, X., Xu, B., 2016. Spatiotemporal pattern of bird habitats in  
854 the Poyang Lake based on Landsat images. *Environ Earth Sci* 75, 1230.  
855 doi:10.1007/s12665-016-5941-6.

856 Yao, J., Zhang, Q., Ye, X., et al., 2018. Quantifying the impact of bathymet-  
857 ric changes on the hydrological regimes in a large floodplain lake: Poyang  
858 Lake. *J Hydrol* 561, 711–723. doi:10.1016/j.jhydrol.2018.04.035.

859 Ye, X., Zhang, Q., Guo, H., Bai, L., 2011. Long-term trend analysis of effect  
860 of the yangtze river on water level variation of poyang lake (1960 to 2007),  
861 in: 2011 International Symposium on Water Resource and Environmental  
862 Protection, IEEE. pp. 543–545.

863 Yin, L., 2010. Integrating 3D Visualization and GIS in Planning Education.  
864 *J Geogr High Educ* 34, 419–438.

865 Yue, T., 2011. Surface modeling: high accuracy and high speed methods.  
866 CRC Press, New York.

867 Yue, T.X., Zhang, L.L., Zhao, N., et al., 2015. "a review of recent de-  
868 velopments in hasm". *Environ Earth Sci* 74, 6541–6549. doi:10.1007/  
869 s12665-015-4489-1.

- 870 Zhao, J., Li, J., Yan, H., et al., 2011. Analysis on the water exchange between  
871 the main stream of the Yangtze River and the Poyang Lake. *Procedia*  
872 *Environ Sci* 10, 2256–2264. doi:10.1016/j.proenv.2011.09.353.
- 873 Zhao, Y., 2018. Simulation analysis platform for the Poyang Lake Basin  
874 Ecosystems, in: *Chinese Water Systems – Poyang Lake*. Springer, pp.  
875 305–318.
- 876 Zhao, Z., 2012. Developing a GIS based Information System for Flood Con-  
877 trol in Poyang Lake Basin. Master’s thesis. Jiangxi Technology University.  
878 In Chinese.
- 879 Zhong, X., 2008. Wetland Data Visualization and Application of Poyang  
880 Lake. Master’s thesis. Jiangxi Normal University. In Chinese.
- 881 Zhou, C., 2018. Bibliometric study of scientific literature on Poyang Lake,  
882 in: *Chinese Water Systems – Poyang Lake*. Springer, pp. 25–40.
- 883 Zhou, L., Hansen, C., 2016. A survey of colormaps in visualization. *IEEE*  
884 *Trans Visual Comput Graph* 22, 2051–2069. doi:10.1109/TVCG.2015.  
885 2489649.
- 886 Zhu, X., 2011. Study on Management System of Poyang Lake Water En-  
887 vironment Based on Open source GIS. Master’s thesis. Nanjing Forestry  
888 University. In chinese.



## 889 List of Figures

890	1	Data life cycle for virtual environments for Earth system mod-	
891		elling. Solid lines mark prevalent types of interfaces, dashed	
892		lines mark plausible but somewhat unusual interfaces. . . . .	42
893	2	a) Location of Poyang Lake and its catchment b) Climograph	
894		for Nanchang City and hydrograph of Poyang Lake at Xingzi	
895		station prior (“Poyang old”) and post the construction of the	
896		Three-Gorges-Dam (Guo et al., 2012; Feng et al., 2016). . . . .	43
897	3	Classification of water quality in Poyang Lake and tributaries	
898		according to the Chinese Environmental Quality Standards for	
899		Surface Water (Jiangxi Water Resources Department, 2013). .	44
900	4	Practical use of the Virtual Reality environment: The user has	
901		zoomed in on the Xin River catchment with the river and its	
902		tributaries visualised in light blue. Flood hydrographs linked	
903		to gauging stations upstream, midstream and downstream (all	
904		marked in white) have been opened for further analysis. . . . .	45
905	5	Results of the hydrodynamic model of Poyang Lake developed	
906		by Du et al. (2018). <b>(a)</b> shows flow direction and velocity of	
907		the lake water using trajectories. Observation sites for meas-	
908		uring water quality (green and purple) as well as eutrophic	
909		sampling sites (orange) are included in the visualisation scene.	
910		<b>(b)</b> visualises the distribution and concentration of total ni-	
911		trogen in the lake. <b>(c)</b> illustrates the variation of inundated	
912		wetland area in Poyang Lake between May (red) and Septem-	
913		ber (yellow). . . . .	46
914	6	Results of the groundwater flow simulation (Nixdorf, 2018). . .	47
915	7	Concentration of various metals in the Gan River network. <b>(a)</b>	
916		Top-down view of the manganese concentration in the river	
917		network. Measurement sites are marked in white. Also vis-	
918		ible is the overlay showing the legend for the included metals,	
919		where green indicates a low concentration, yellow the recom-	
920		ended limit for drinking water and red the critical concen-	
921		tration for drinking water. <b>(b)</b> Isometric view westward from	
922		Poyang Lake (visible at the bottom). Colours indicate the lead	
923		concentration. Cones are marking coal- (black), iron- (light	
924		blue) and tungsten-mines (dark blue) located in the region. . .	48

925	8	Data life cycle for Virtual Environments for Earth system	
926		modelling. . . . .	49
927	9	Exemplarily application of data integration for Le'an River:	
928		(a) The original dataset is georeferenced to fit the geographic	
929		context, (b) unneeded points are removed from the dataset and	
930		polylines are mapped to the digital elevation model (shown	
931		here is a $40\times$ super-elevation to illustrate the effect), (c) the	
932		dataset is stylised as a tube to be easily visible within the con-	
933		text and given an intuitive colour. Data representing copper-	
934		concentration in the river is added and subsequently visualised	
935		using a manually adjusted transfer function. . . . .	50
936	10	Visualisation of rain events via a time series of point clouds	
937		derived form meteorological raster data. Two approaches have	
938		been tested: a simple rendering of points is shown in figs. (a)	
939		and (b), whereas points have been rendered as small discs in	
940		fig. (c). . . . .	51
941	11	Visualisation of sensor measurements via on-line access to the	
942		AL.VIS/Timeseries framework. . . . .	52
943	12	Data analysis of groundwater and lake data in the virtual real-	
944		ity environment. . . . .	53

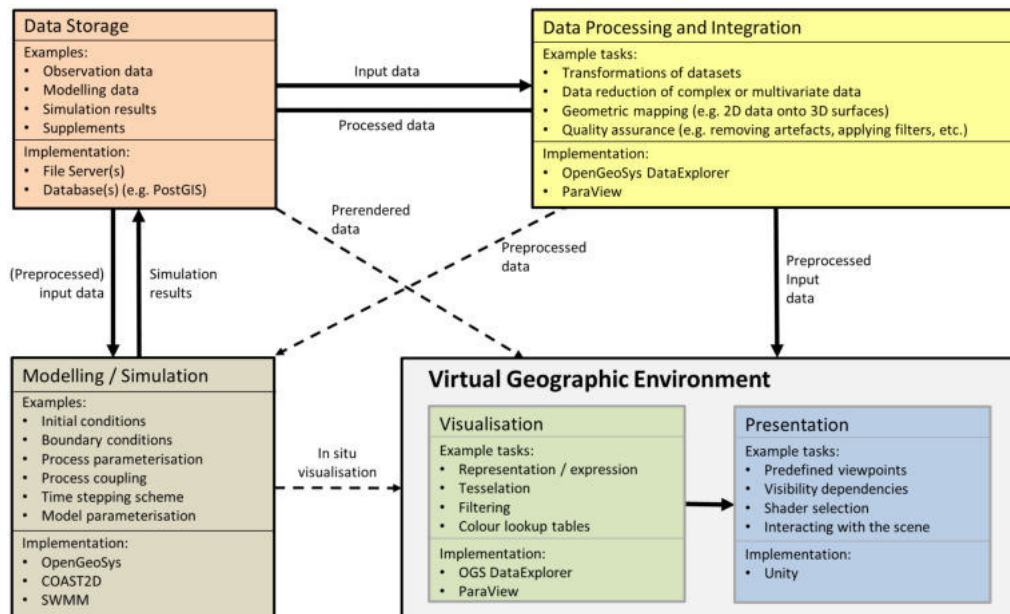


Figure 1: Data life cycle for virtual environments for Earth system modelling. Solid lines mark prevalent types of interfaces, dashed lines mark plausible but somewhat unusual interfaces.

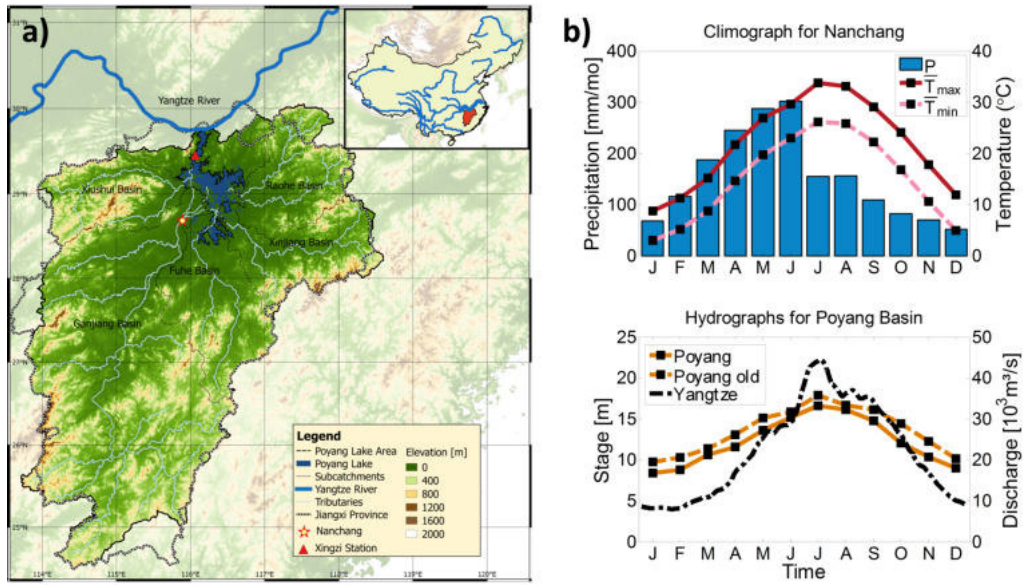


Figure 2: a) Location of Poyang Lake and its catchment b) Climograph for Nanchang City and hydrograph of Poyang Lake at Xingzi station prior (“Poyang old”) and post the construction of the Three-Gorges-Dam (Guo et al., 2012; Feng et al., 2016).

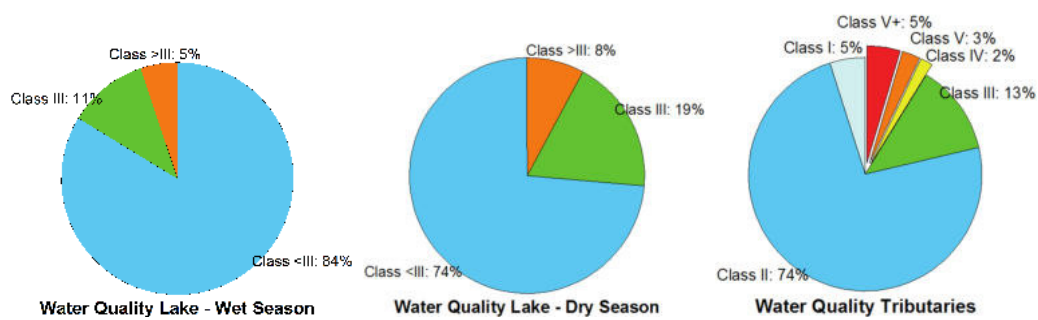


Figure 3: Classification of water quality in Poyang Lake and tributaries according to the Chinese Environmental Quality Standards for Surface Water (Jiangxi Water Resources Department, 2013).



Figure 4: Practical use of the Virtual Reality environment: The user has zoomed in on the Xin River catchment with the river and its tributaries visualised in light blue. Flood hydrographs linked to gauging stations upstream, midstream and downstream (all marked in white) have been opened for further analysis.

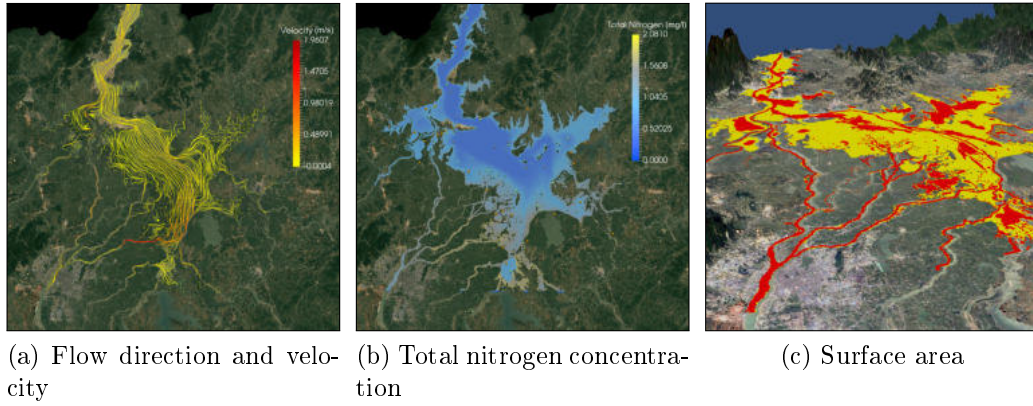
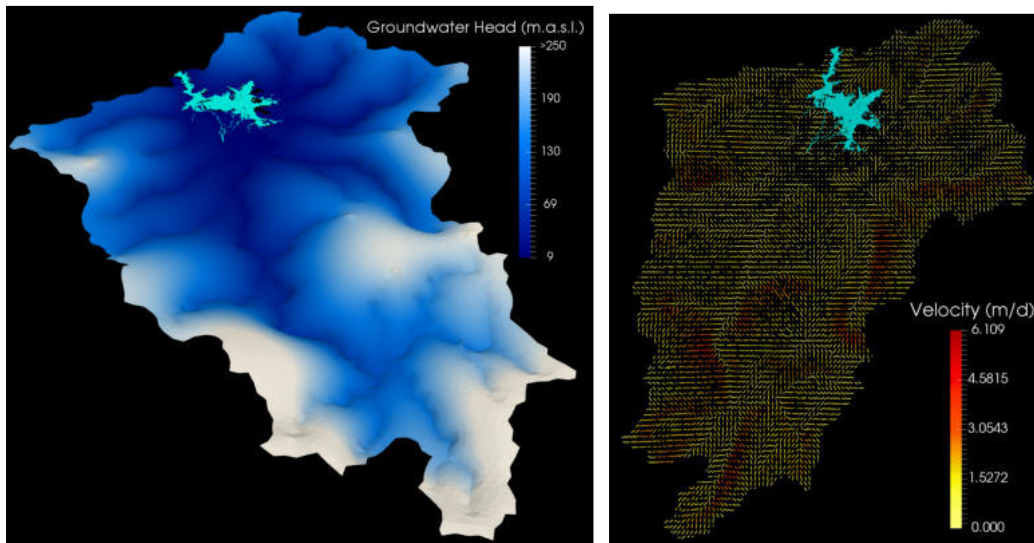
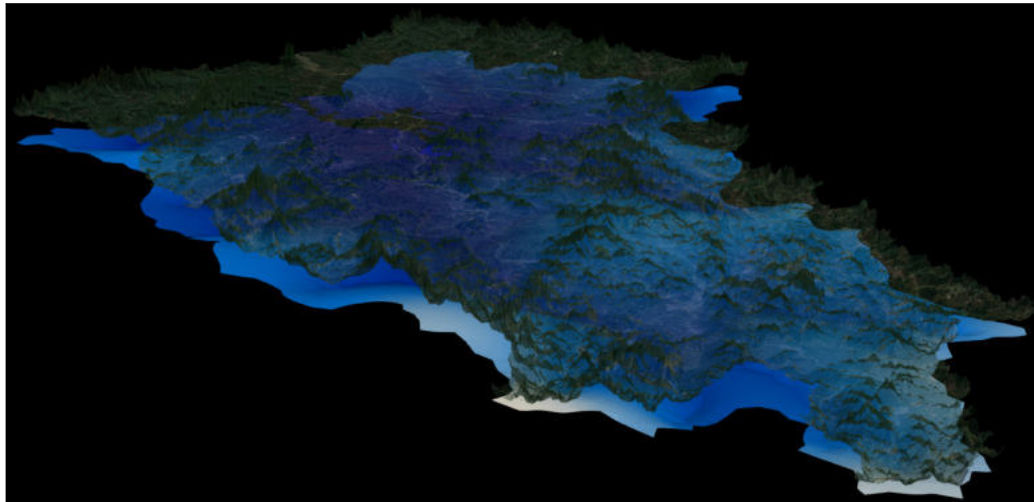


Figure 5: Results of the hydrodynamic model of Poyang Lake developed by Du et al. (2018). **(a)** shows flow direction and velocity of the lake water using trajectories. Observation sites for measuring water quality (green and purple) as well as eutrophic sampling sites (orange) are included in the visualisation scene. **(b)** visualises the distribution and concentration of total nitrogen in the lake. **(c)** illustrates the variation of inundated wetland area in Poyang Lake between May (red) and September (yellow).



(a) Groundwater head (superelevated)

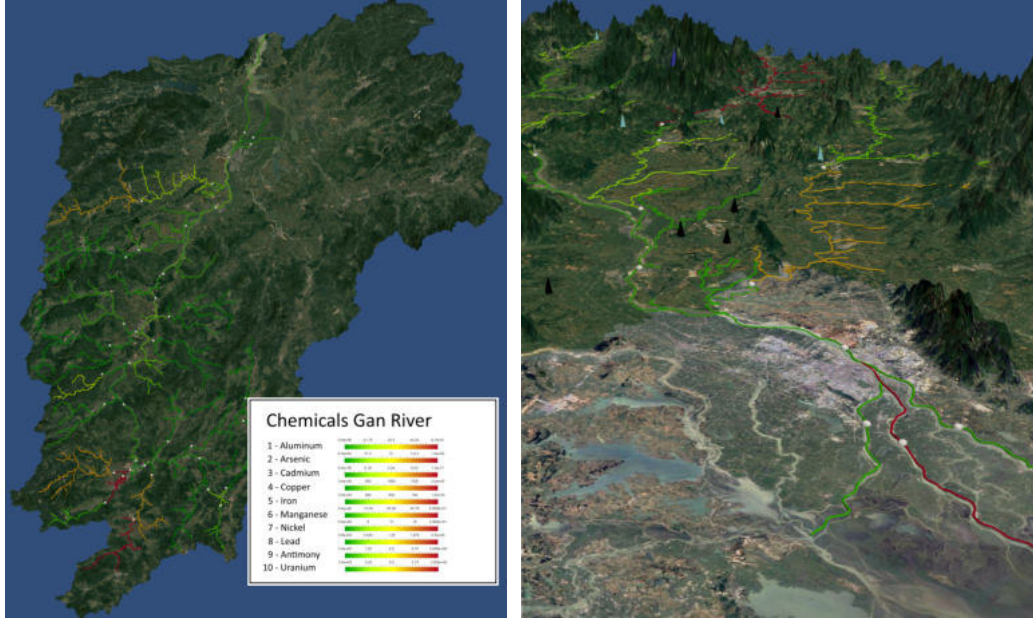
(b) Groundwater flow and velocity



(c) Combined visualisation of groundwater head and surface data

Figure 6: Results of the groundwater flow simulation (Nixdorf, 2018).





(a) Manganese concentration

(b) Lead concentration

Figure 7: Concentration of various metals in the Gan River network. **(a)** Top-down view of the manganese concentration in the river network. Measurement sites are marked in white. Also visible is the overlay showing the legend for the included metals, where green indicates a low concentration, yellow the recommended limit for drinking water and red the critical concentration for drinking water. **(b)** Isometric view westward from Poyang Lake (visible at the bottom). Colours indicate the lead concentration. Cones are marking coal- (black), iron- (light blue) and tungsten-mines (dark blue) located in the region.

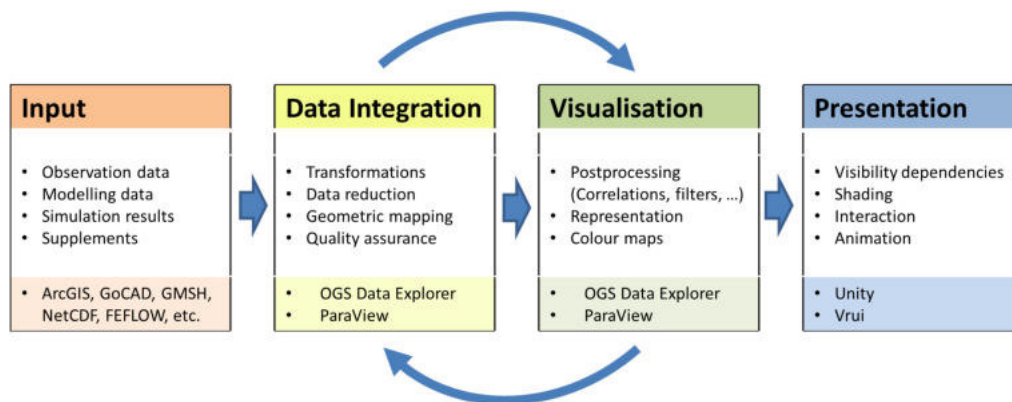


Figure 8: Data life cycle for Virtual Environments for Earth system modelling.

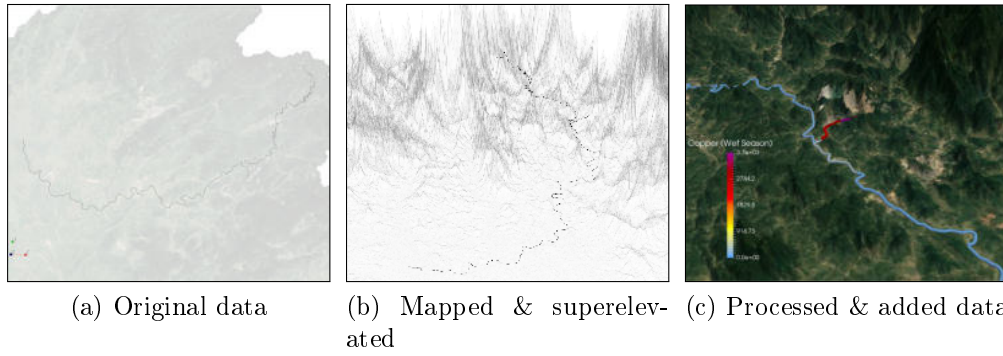


Figure 9: Exemplarily application of data integration for Le'an River: (a) The original dataset is georeferenced to fit the geographic context, (b) unneeded points are removed from the dataset and polylines are mapped to the digital elevation model (shown here is a  $40\times$  super-elevation to illustrate the effect), (c) the dataset is stylised as a tube to be easily visible within the context and given an intuitive colour. Data representing copper-concentration in the river is added and subsequently visualised using a manually adjusted transfer function.

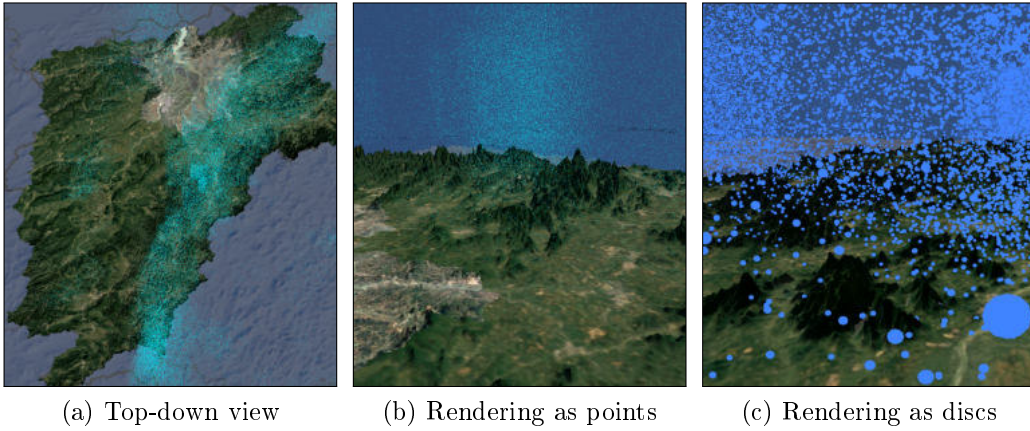


Figure 10: Visualisation of rain events via a time series of point clouds derived from meteorological raster data. Two approaches have been tested: a simple rendering of points is shown in figs. (a) and (b), whereas points have been rendered as small discs in fig. (c).

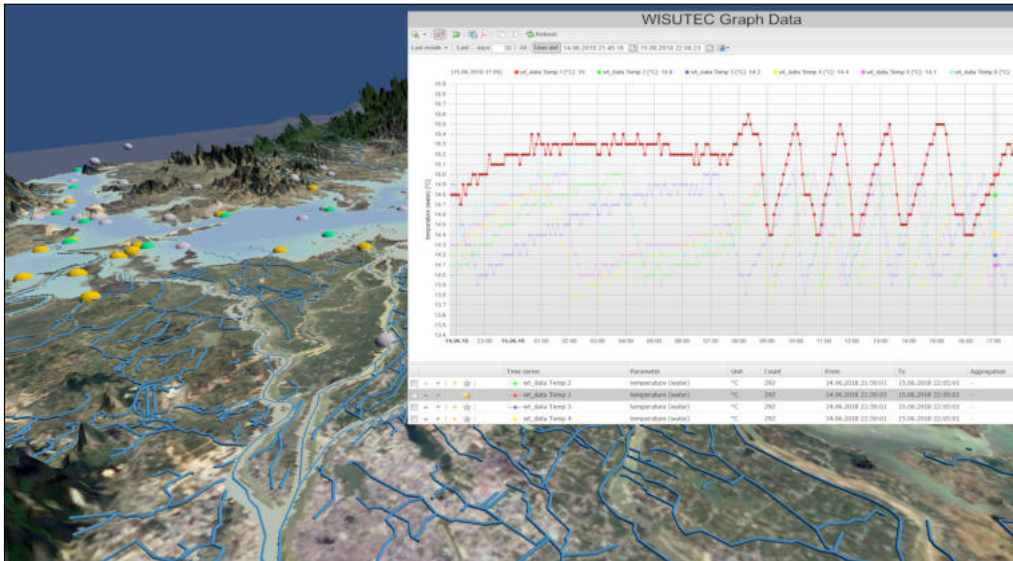


Figure 11: Visualisation of sensor measurements via on-line access to the AL.VIS/Timeseries framework.

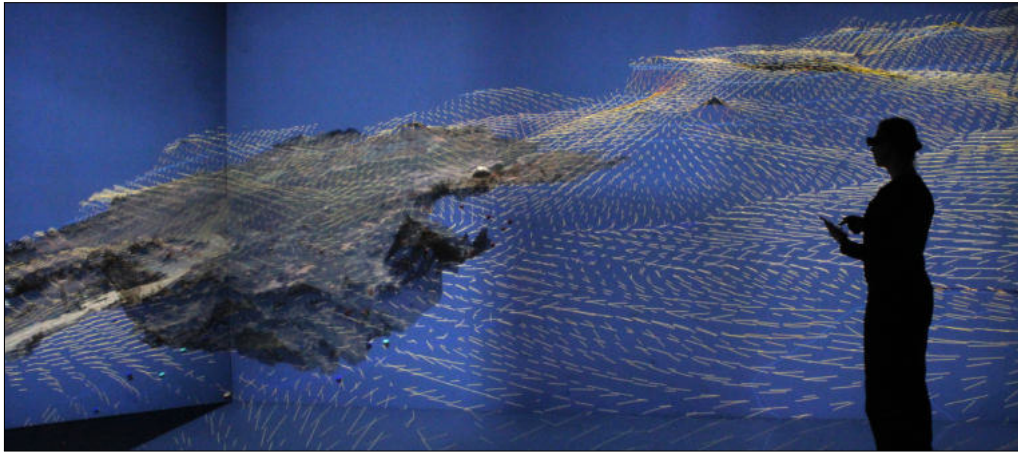


Figure 12: Data analysis of groundwater and lake data in the virtual reality environment.